CrossMark

Thermal properties of n-pentadecane, n-heptadecane and n-nonadecane in the solid/liquid phase change region

Catalina Vélez, José M. Ortiz de Zárate[*], Mohamed Khayet

Department of Applied Physics I, Faculty of Physics, University Complutense of Madrid, Avd. Complutense s/n, 28040 Madrid, Spain

A R T I C L E   I N F O

A B S T R A C T

The thermal properties including the thermal conductivity (λ), the specific heat (c_p), the melting and crystallization temperatures together with their corresponding transition heat enthalpies of the odd-numbered linear alkane hydrocarbons n-pentadecane, n-heptadecane and n-nonadecane were measured in both the solid and liquid phases using the transient hot wire and the differential scanning calorimetry (DSC) techniques. The obtained results were compared with available literature data. Discussions were based also on the X-ray diffraction spectra of the three n-alkanes carried out at different temperatures and including both solid and liquid phases. A discontinuity of λ is observed at the solid - liquid phase transition of the three n-alkane hydrocarbons.

1. Introduction

Linear alkanes (C_nH_{2n+2}) with carbon number (n) between 12 and 40 are generically known as paraffins. At atmospheric pressure, paraffins have a solid/liquid melting point that is around ambient temperatures, with a relatively high melting enthalpy. Hence, paraffins are being employed as the main component of the so-called Phase Change Materials (PCM), that are nowadays used for improving heat transfer in many thermal processes, and for energy storage [1,2]. PCMs have been an active research field in last years, most recent developments include, for instance, the addition of nanoparticles to further enhance their heat transfer properties [3,4].

For an efficient design of processes that use PCM in heat transfer, heat recovery or energy storage, it is essential to know accurately the thermophysical properties, for extended temperature intervals, of the linear alkanes at the base of their formulation [2]. Specifically, reliable values of the enthalpy of melting (ΔH_m), the isobaric specific heat (c_p) and the thermal conductivity (λ) are required. Experimental data for the ΔH_m and c_p of most linear n-alkanes are accesible in standard compilations, such as the NIST Chemistry Webbook [5]. In contrast, very few dedicated experimental studies of the λ of n-alkanes and commercial paraffins have been published so far in refereed scientific sources. Moreover, most of them are already rather old, and only report data for the solid or for the liquid phase, not for solid and liquid including the phase transition region and using the same set-up. For these reasons, we are carrying out a program [6] to measure thermophysical properties of n-alkanes (including λ) at atmospheric pressure and over extended temperature intervals that, for each alkane, contain the corresponding melting temperature, T_m.

The present paper presents the thermal properties of three odd-numbered n-alkanes, namely, n-pentadecane, n-heptadecane and n-nonadecane. It is known [5,7] that these odd-numbered alkanes at atmospheric pressure present two different solid phases. Precipitation of paraffins in pipelines is a major problem in the petrochemical industry and many studies [8–14] have been devoted to the thermodynamic and structural properties of their solid phases, even a comprehensive review exists [7]. The three n-alkanes considered here exhibit [7] a *Pbcm* orthorhombic crystal structure at low temperature [7,10,11]. With increasing temperature the structure becomes *Fmmm* orthorhombic and presents orientational disorder [7], being referred to as rotator structure by some authors [10,11,13]. Finally, with further temperature increase the liquid phase (L) is reached. Following the nomenclature of Dirand

* Corresponding author.
E-mail addresses: jmortiz@fis.ucm.es (J.M. Ortiz de Zárate), khayetm@fis.ucm.es (M. Khayet).

et al. [7] we shall refer here to the lower temperature solid phase as 'Ordered Solid (OS)', while the intermediate solid phase shall be referred to as 'Disordered Solid (DS)'. The corresponding two phase transitions are 'od' for ordered solid to disordered solid, and melting (m) for disordered solid to liquid. For the three alkanes investigated here, the transition temperatures T_{od} and T_m are relatively close [5,7], leading to a complex melting behavior, that might provide a well-defined model system for studying the sometimes complicated crystallization of polymers, surfactants, lipids, etc [14,15].

For λ measurements, the transient hot-wire technique was used. The advantage of this technique is that the same set-up can be employed, irrespective of the material under test being in the solid or in the liquid phase. The transient hot-wire technique is nowadays well established to measure λ of electrically nonconducting solids, fluids and nanofluids, giving very reproducible values with uncertainties that can be below 1% for most of the systems [16]. With the exception of the critical region and the very low pressure region for gases, the transient hot-wire technique has been employed successfully for wide temperature and pressure intervals. For our purposes the transient hot-wire is advantageous as compared to a flash method (that measures directly the thermal diffusivity) or to commercial hot-disks (that require liquids to be placed inside a vessel).

For further characterization of the samples, DSC and X-ray diffraction (XRD) tests were performed, from which more detailed information was obtained about the complex phase transition exhibited by these n-alkanes, that is helpful for the interpretation of the obtained λ values. From the analysis of DSC curves, the transition temperatures, the corresponding enthalpies of transition, and the specific heat at the solid and liquid phases were determined. From XRD patterns, the structure constants of the two crystalline phases exhibited by the studied n-alkanes were estimated.

2. Experimental methods

2.1. Materials

The chemicals were purchased from Sigma-Aldrich and were used as supplied, without further purification. n-pentadecane ($CH_3(CH_2)_{13}CH_3$, CAS 629-62-9, catalog# P3406), n-heptadecane ($CH_3(CH_2)_{15}CH_3$, CAS 629-78-7, catalog# 128503), and n-nonadecane ($CH_3(CH_2)_{17}CH_3$, CAS 629-92-5, catalog# N28906) all have a nominal purity of 99%.

2.2. Instruments

The DSC measurements were carried out with a DSC1 instrument (Mettler Toledo). Indium was used as standard reference for the calibration. The samples were sealed in aluminium pans, the masses being typically 5.8 mg for the n-pentadecane, 6.5 mg for the n-heptadecane and 10.1 mg for the n-nonadecane. Both heating (melting) and cooling (crystallization) curves were registered between 258 K and 348 K with a linear increase of temperature of 2 K/min. All runs were performed under a constant stream of nitrogen and at atmospheric pressure. As further explained below, transition temperatures, enthalpies of transition and specific heats were obtained from the analysis of DSC curves, for which the software STAR^e was used.

For the XRD measurements a X'Pert PRO MPD instrument (Panalytical) was used in the th—th configuration, equipped with an Oxford—Phoenix low temperature camera. All measured diffractograms were obtained with the same range, optics, size and time step. Samples were placed in a copper—chromium holder under

vacuum, then cooled at 1 K/min up to 261 K. Subsequently, while the temperature of the holder increased at 0.5 K/min, XRD diffractograms were obtained every 2 K until the sample melting temperature was reached. Data was normalized with the XPert HighScore software (Panalytical), after which the position and shape of the different peaks were obtained by fitting to pseudo-Voigt functions. Finally, from the peak positions, the structure was analyzed and the corresponding constants were obtained with the help of the *Fullprof Suite* software.

The thermal conductivity (λ) was measured with a versatile custom transient hot-wire calorimeter developed in our laboratory, which has been applied successfully to measure $\lambda(T)$ of pure liquids [17], nanofluids [18], clays [19] and even-numbered paraffins [6]. The apparatus configuration and data reduction process adopted for the present investigation were essentially the same as in the preceding researchs [18,19]. The core of the apparatus is a platinum wire of 50 μm diameter and about 20 cm length. Since the wires usually break up after some weeks of continuous use and temperature cycling, three different wires with slightly different lengths, were actually employed for the measurements reported in this study. The wire is mounted in a plastic frame to keep it straight. The frame with the wire is placed inside a measurement cell filled with the sample in liquid state. The temperature of the measurement cell is controlled by a combination of a circulation bath and a controlled atmosphere chamber. For the present study, the used bath is Lauda ECO RE630, which permits to establish the required temperature in a wide range and control. Once temperature is stabilized, measurements are performed by circulating through the wire an electrical current of known intensity I while acquiring readings of the voltage drop $V(t)$ along the wire as a function of time. For the electrical measurements, a Keithley 2400 source meter interfaced to a computer was employed. The theory of the hot-wire calorimetry [20,21] indicates, after a short transient, a linear increase of V with $\ln t$

$$V(t) = a + b\ln t, \tag{1}$$

where, in practice, a and b are two fitting parameters. Our previous experience with this set-up [18,19] shows that, from a given run i, an individual value for the thermal conductivity λ_i can be calculated by

$$\lambda_i = A\frac{I_i^3 R_{0,i}}{b_i}, \tag{2}$$

where I_i is the current intensity used for the run, $R_{0,i}$ is the electrical resistance measured just before switching on the current source (that depends on temperature at which the run is performed), and b_i is the slope obtained by fitting the corresponding $V(t)$ curve to Eq. (1). Finally, A in Eq. (2) represents a calibration constant that depends on the wire geometry and on the slope of the linear relationship between the electrical resistance of the platinum wire and temperature; but not on the current I_i, neither on the (initial) temperature at which the run is performed. In practice [18,19], A was obtained for each one of the three wires used in this research following the ASTM-D2717 standard, carrying out preliminary measurements with water and dimethylphalate covering the same temperature range at which the n-alkanes were later tested. Additional measurements with water after measuring the n-alkanes are performed to check the A value and, hence, the stability of the system. Notice that the constant A also includes all the sources of systematic errors in the λ measurements. Previous detailed analysis [18,19] yielded that the uncertainty associated with the calibration procedure (and, hence, to the constant A) is $\pm 3\%$. This
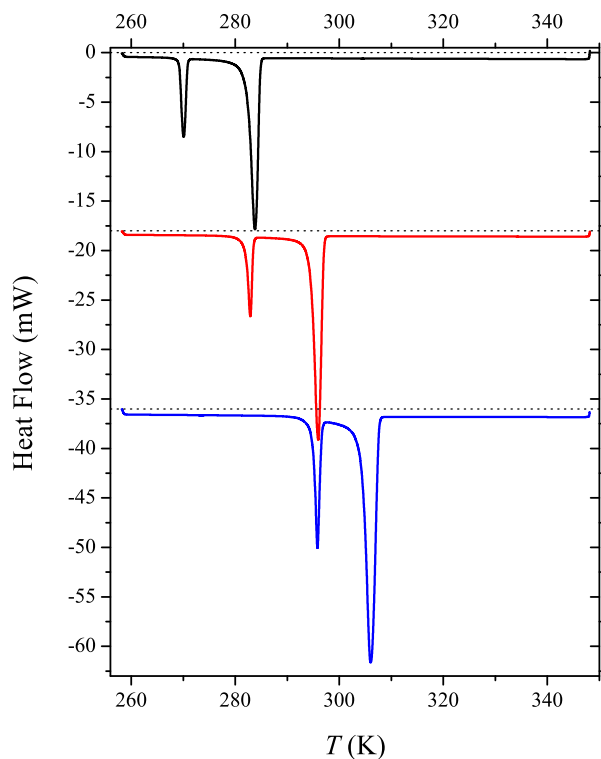
Fig. 1. Melting DSC curves for n-pentadecane (top, black), n-heptadecane (middle, red) and n-nonadecane (bottom, blue). For clarity, the ordinate of n-heptadecane was moved to −18 mW and the ordinate of n-nonadecane to −36 mW, indicated as dotted lines. In each case, two prominent peaks are clearly visible, corresponding to the OS-DS (lower temperature) and DS-L (higher temperature) phase transitions. (For interpretation of the references to colour in this figure legend, the reader is referred to the web version of this article.)

Table 1
Results of the analysis of DSC curves. Temperatures of phase change and corresponding enthalpies of transition. Only data obtained from the analysis of heating curves (melting) is presented.

	Heating (melting)			
	Ordered solid − disordered solid		Disordered solid − liquid	
Alkane	T_{od} (K)	ΔH_{od} (kJ/mol)	T_m (K)	ΔH_m (kJ/mol)
n-pentadecane	269.25 ± 0.01	8.88 ± 0.02	282.30 ± 0.01	34.62 ± 0.01
n-heptadecane	281.96 ± 0.06	9.64 ± 0.12	294.47 ± 0.01	39.68 ± 0.15
n-nonadecane	294.97 ± 0.01	11.20 ± 0.03	304.37 ± 0.01	44.61 ± 0.08

long-time non-linearities appearing in $\{V(t), \ln t\}$ plots. This was checked throughout all measurements.

3. Experimental results

3.1. DSC

As an example of the DSC measurements we show in Fig. 1 experimental melting curves obtained for one sample of n-pentadecane, one sample of n-heptadecane and one sample of n-nonadecane. What is first evident in Fig. 1 is the presence, for each one of the investigated n-alkanes, of two close but different peaks that indicate the existence of two distinct solid phases [5,7–13,26]. The lower temperature peak corresponds to the 'od' phase transition and the higher temperature peak to melting.

From DSC curves, with the help of the STAR^e software, the transition temperatures and the corresponding enthalpies of transition are readily obtained. The transition temperatures (T_{od} for OS-DS and T_m for DS-L) are determined as the onset of the DSC peaks. To obtain them the STAR^e software traces a straight line at the point of maximum slope of the leading edge of the peak and extrapolates to baseline. STAR^e determines the latent heats (ΔH_{od} for OS-DS and ΔH_m for DS-L) by a numerical integration of area under the peaks that represent each of the phase transitions, after baseline substraction. The results obtained from such an analysis are summarized in Table 1. For each of the linear alkanes three different DSC runs were performed, with slightly different sample masses. The data in Table 1 are the average of the values obtained from each of the three runs for each n-alkane, while uncertainties in Table 1 correspond to standard deviations. We only report in Table 1 the values obtained from the heating (melting) runs, that are free from supercooling or metastability. Indeed, as usual [27], likely because of metastability, one systematically observes a certain difference between the temperatures at which the peaks are centered when cooling and the temperatures at which the peaks are centered when heating.

The results reported in Table 1 agree well, within 1%, with standard references and data compilations such as the NIST webbook [5] or Table 2 in Dirand et al. [7]. The results reported in Table 1 also agree well with other measurements [10,12] not

uncertainty should be added (in quadrature) to the random errors discussed later.

For the results presented in this paper, for each n-alkane and each temperature, 275 individual λ_i measurements were obtained at various electrical currents between 160 mA and 260 mA. Individual heating runs were performed with a waiting time of 4 min between consecutive runs, being the whole data acquisition process time about 18 h. All these data were reduced to a single $\lambda(T)$ for each n-alkane, with its corresponding random error $\Delta\lambda$, by gaussian fittings described in detail elsewhere [19]. The temperatures inside the cell were measured with a platinum resistance thermometer, and the temperature corresponding to each $\lambda(T)$ was obtained by averaging over individual readings (usually within ±0.05 K). Once the measurements at a given T were finished, a new temperature was set, and the whole process was repeated. Measurements were done at atmospheric pressure, which at our location it usually fluctuates around 925 mbar. It is worth mentioning that solidification of the sample occurs inside the measurement cell (as temperature is lowered), and that the data acquisition and reduction procedure to determine $\lambda(T)$ were exactly the same, regardless of the sample being in the solid or in the liquid state.

To reliably obtain λ from Eqs. (1)–(2) convection must be absent in the system. Hence, we adjusted the duration of the heating runs to 1.6 s, corresponding to a Fourier number Fo ≃ 250, since previous numerical and experimental studies [22–25] indicated that convection was not present in this range of Fo. From the proposed empirical correlations in Refs. [22,23] we estimate that convection would appear in our system at approximately 8–10 s after the heating starts, a fact that we have also verified experimentally as

Table 2
Parameters A and B obtained from fitting the c_p experimental data points to Eq. (3). For each n-alkane and thermodynamic phase, the temperature range in which the parameters are valid is also indicated. With the reported parameters, the measured experimental data are represented within ± 2%, that is around the estimated uncertainty of the data themselves.

Paraffin	Phase	A (J g^{-1} K^{-2})	B (J g^{-1} K^{-1})	Range, T in K
n-pentadecane	liquid	0.00257	1.45473	$300 \leq T \leq 334$
n-heptadecane	ordered solid	0.01731	−2.8123	$265 \leq T \leq 270$
n-heptadecane	liquid	0.00367	1.1136	$306 \leq T \leq 334$
n-nonadecane	ordered solid	0.01055	−1.0807	$265 \leq T \leq 280$
n-nonadecane	liquid	0.00313	1.27732	$316 \leq T \leq 334$

included in these compilations. In addition, T_{od} in Table 1 agree well with the temperatures reported by Doucet *et al* [11] for the OS-DS phase transition obtained from XRD, *i.e.*, 283.15 K for the n-heptadecane [11] and 293.15 K for the n-nonadecane [11]. An intriguing fact that can be noticed in Table 1, and also quite clearly in Fig. 1, is the almost exact match between the OS-DS transition temperature for n-heptadecane and the DS-L transition temperature for n-pentadecane. Similar coincidence is detected between the OS-DS transition temperature for n-nonadecane and the DS-L transition temperature for n-heptadecane. We don't have an explanation yet for this fact, and we do believe it may be worthy of further investigation.

From the analysis of DSC curves, c_p can also be measured. Actually, c_p values can be obtained only for the temperature ranges that appear as almost flat in plots like Fig. 1. This means that one has to crop the peaks corresponding to the two phase transitions. Although may be not fully evident in Fig. 1 because of the scale, it turns out that the DSC peaks corresponding to the two phase transitions display quite long tails, that strongly reduce the temperature range where reliable c_p measurements by DSC are possible. To alleviate this problem, we have performed DSC runs specifically aimed to the measurement of c_p with a larger linear temperature increase of 5 K/min. In spite of this, one cannot obtain reliable c_p values inside a temperature interval of about ±12 K around the center of the two phase transition peaks. Consequently, in no case could we obtain reliable c_p values for the intermediate DS phase, and for the n-pentadecane we were even not able to get reliable c_p values for the OS phase. Accounting for these limitations, we show in Fig. 2 the c_p values that we were able to measure for the three investigated n-alkanes, together with some reference

literature data [28—32]. Our current measurements are represented with solid circles, but they are so numerous that they appear as thick solid lines in Fig. 2. We observe good agreement of the current c_p measurements with literature data. It is worth quoting the lack of data published in refereed scientific journals, particularly for the solid phases, OS and DS. Most of the quoted literature values were obtained with adiabatic calorimeters, so that they are free from the inherent limitations of the DSC method when performing c_p measurements close to a phase transition.

To numerically report the current c_p measurements, we found convenient to fit the experimental points in Fig. 2 to linear temperature dependence

$$c_p = AT + B. \tag{3}$$

This linear fit represents the experimental data within ±2%, that is the estimated uncertainty of the data themselves. Hence, we display in Table 2 the parameters A and B obtained from these fittings for the different n-alkanes and thermodynamic phases together with the corresponding temperature ranges (temperatures in K).

3.2. XRD

X-ray difractograms of the n-alkanes in the solid phases were obtained as a function of temperature. For the three samples, X-ray diffractograms were measured starting at 261 K, and up to 273 K for n-pentadecane, 291 K for n-heptadecane and 303 K for n-nonadecane. Fig. 3 shows, as an example, three difractograms obtained for n-pentadecane at three different temperatures. The two difractograms corresponding to the solid phases display two prominent peaks, while the diffractogram corresponding to the liquid phase is featureless, typical of an amorphous material.

Previous XRD studies of long-chain n-alkanes include Craig *et al* [14], who used high resolution synchrotron radiation at a single temperature for each substance. Craig *et al* [14] determined the solid structure of these three n-alkanes to be orthorhombic, with angles $\alpha=\beta=\gamma=90°$. Similarly, Metivaud *et al* [10] confirm the orthorhombic structure at lower temperatures, while finding some orientational disorder at the crystalline II solid phase. Hence, in the present study the X-ray diffractograms as those shown in Fig. 3 were analyzed assuming orthorhombic structure, and
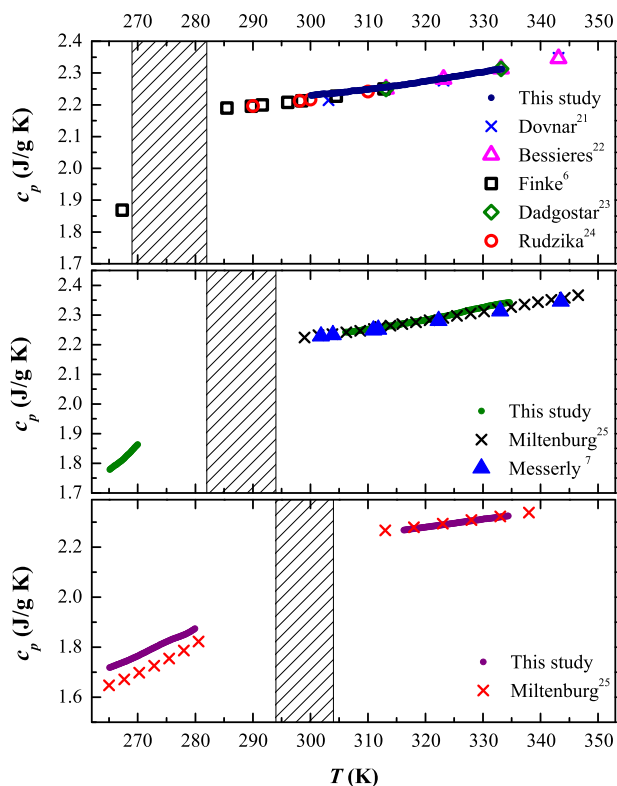

Fig. 2. Isobaric specific heat capacity measured in this research (solid circles) for n-pentadecane (top panel) n-heptadecane (middle panel) and n-nonadecane (bottom panel). The number of points is large, so that they appear as continuous thick curves. Literature values, as indicated, are added with different symbols. The patterned area corresponds, in each case, to the DS phase (between the two observed DSC peaks).
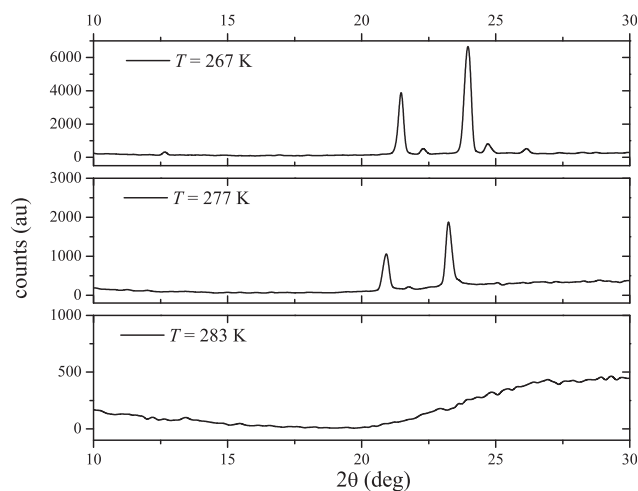

Fig. 3. Diffractograms measured for the n-pentadecane, at various temperatures as indicated. The upper panel corresponds to the OS phase, the middle panel to the DS phase and the lower panel to the liquid phase. From the peaks displayed at solid state the parameters of the unit cell were calculated.
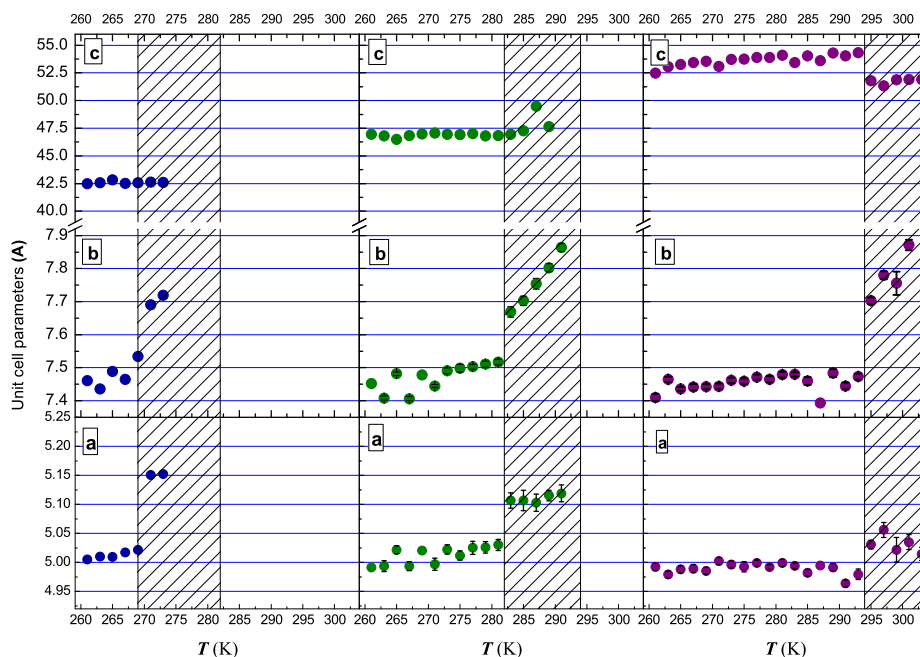
Fig. 4. Unit cell parameters *a* (lower panel), *b* (middle panel) and *c* (upper panel) in Å, as a function of temperature, for n-pentadecane (left column) n-heptadecane (middle column) and n-nonadecane (right column). The patterned area corresponds, in each case, to the DS phase (between the two observed DSC peaks).

determining the dimensions of the unit cell (parameters *a*, *b* and *c*) by means of the *Fullprof Suite* software. The results are plotted in Fig. 4 as a function of temperature, for the three investigated n-alkanes. For clarity, we have patterned the temperature range corresponding to the disordered solid (DS) intermediate solid phase, as measured by DSC. A quick look at Fig. 4 shows that the unit cell parameter *c* is, more or less, independent of temperature, while parameters *a* and *b* appear to show a discontinuity at the transition between the two solid phases. Hence, structural changes associated with the OS - DS phase change have been detected.

To quantitatively compare with reference data, we have averaged the values measured at the lower temperature phase (OS) since Fig. 4 shows that the three parameters of the orthorhombic unit cell are nearly independent of temperature inside this region. Table 3 reports these averages with uncertainties obtained as standard deviations. Some data published in refereed scientific journals is also displayed in the second part of Table 3, and reasonable agreements are found with the current values. It should be noted that the current values in Table 3 represent an average over several temperatures in the ordered solid OS region, while literature data are for a single temperature: around 298 K for n-nonadecane [14,33], 264 K for n-pentadecane [14] and 278 K for n-heptadecane [14]. Poorer agreement is found with the data of

Larsson [13], that refer to the DS solid phase while our current data are for the OS phase. In addition, the measured values for the *c* parameter of the unit cell are consistent with the empirical correlation proposed by Broadhurst [7,34].

In addition to the literature data reported in Table 3, Doucet *et al* [11] also measured the unit cell parameters as a function of temperature for n-heptadecane and n-nonadecane, although they only show the results graphically. The values obtained in the present study compare well with those of Doucet *et al* [11].

3.3. Thermal conductivity

For each investigated n-alkane two measurement series were done. The first was from lower to higher temperature and the second from higher to lower temperature. The reported λ values are an average of the two series. Programmed temperatures in the circulation bath ranged from 258 K to 333 K, with steps of 10 K. Table 4 summarizes the results for λ(T) including values for both the ordered solid phase and the liquid phase. For clarity, and for each n-alkane, a horizontal line separates measurements in the solid state from measurements in the liquid state. The uncertainty indicated in Table 4 for the λ measurements represents the random errors only, and it was obtained by the same gaussian statistical analysis used

Table 3
Orthorhombic unit cell parameters for n-pentadecane, n-heptadecane and n-dodecane measured in this study (uncertainties are standard deviations) for the ordered solid (OS) phase, and some literature reference values.

Paraffin	*a* (Å)	*b* (Å)	*c* (Å)	Reference
n-pentadecane	5.010 ± 0.005	7.462 ± 0.022	42.61 ± 0.16	Present study
n-heptadecane	5.012 ± 0.015	7.472 ± 0.039	46.88 ± 0.16	
n-nonadecane	4.992 ± 0.013	7.467 ± 0.063	53.54 ± 0.64	
n-pentadecane	5.079 ± 0.021	7.535 ± 0.018	42.125 ± 0.148	Craig *et al* [14]
n-heptadecane	4.972 ± 0.002	7.460 ± 0.002	46.898 ± 0.008	
n-nonadecane	5.038 ± 0.001	7.666 ± 0.001	52.245 ± 0.007	
	4.975 ± 0.001	7.458 ± 0.001	51.999 ± 0.0007	Gerson *et al* [33]
	4.79 ± 0.05	8.30 ± 0.08	52.8 ± 0.05	Larsson [13]

Table 4

Thermal conductivity of n-pentadecane, n-heptadecane and n-nonadecane at various temperatures, as indicated. The uncertainty shown for the λ values corresponds to random errors only, a systematic error contribution estimated in ±3% should be added. For each alkane, a horizontal line separates measurements in the ordered solid (OS) state from measurements in the liquid state.

n-pentadecane, $CH_3(CH_2)_{14}CH_3$
T (K)	λ (W/m K)	T (K)	λ (W/m K)
258.84	0.186 ± 0.007	303.53	0.143 ± 0.003
261.28	0.184 ± 0.011	308.78	0.141 ± 0.003
262.17	0.182 ± 0.015	315.56	0.140 ± 0.003
283.61	0.147 ± 0.002	318.48	0.141 ± 0.003
288.60	0.146 ± 0.003	323.51	0.139 ± 0.003
293.50	0.144 ± 0.003	328.40	0.139 ± 0.003
298.57	0.143 ± 0.003	333.47	0.138 ± 0.005

n-heptadecane, $CH_3(CH_2)_{16}CH_3$
T (K)	λ (W/m K)	T (K)	λ (W/m K)
258.82	0.202 ± 0.005	303.35	0.146 ± 0.003
261.26	0.205 ± 0.004	308.37	0.146 ± 0.003
263.83	0.203 ± 0.004	313.45	0.144 ± 0.002
266.24	0.200 ± 0.004	318.47	0.143 ± 0.003
268.61	0.203 ± 0.005	323.40	0.143 ± 0.002
271.07	0.200 ± 0.005	328.36	0.142 ± 0.002
273.49	0.197 ± 0.007	333.33	0.143 ± 0.003
298.34	0.146 ± 0.002		

n-nonadecane, $CH_3(CH_2)_{18}CH_3$
T (K)	λ (W/m K)	T (K)	λ (W/m K)
258.84	0.226 ± 0.004	280.90	0.215 ± 0.004
261.28	0.224 ± 0.004	283.37	0.213 ± 0.005
263.62	0.222 ± 0.004	305.94	0.152 ± 0.002
266.18	0.218 ± 0.004	308.39	0.152 ± 0.003
268.56	0.219 ± 0.005	313.38	0.151 ± 0.003
271.05	0.214 ± 0.005	318.48	0.150 ± 0.003
273.53	0.216 ± 0.004	323.51	0.149 ± 0.003
275.48	0.217 ± 0.004	328.43	0.147 ± 0.003
278.45	0.215 ± 0.004	333.48	0.148 ± 0.003

elsewhere [19]. As it was mentioned above, we estimate our data to be affected by an additional ±3% of systematic error, that has to be (quadratically) added in the final error. Table 4 shows that, in general, the data corresponding to the solid phase have a larger uncertainty than the data corresponding to the liquid phase.

It is worth mentioning that the theory of hot-wire used for data reduction assumes that all the heat generated in the wire by Joule effect is dissipated by conduction through the surrounding sample. Obviously, this is not true for the data obtained at (initial)
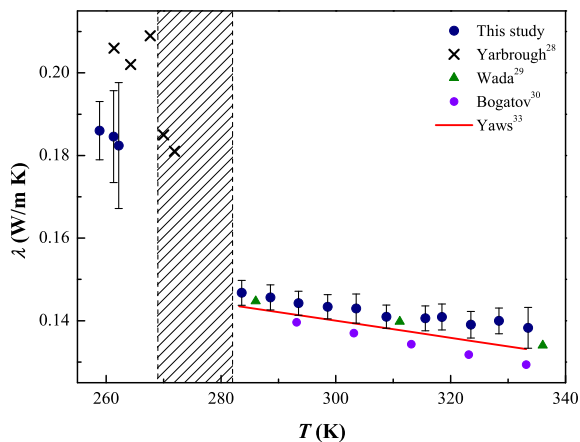
Fig. 6. Thermal conductivity measured for n-heptadecane as a function of the temperature, together with available literature data as indicated. The patterned area corresponds to the DS phase (between the two observed DSC peaks).
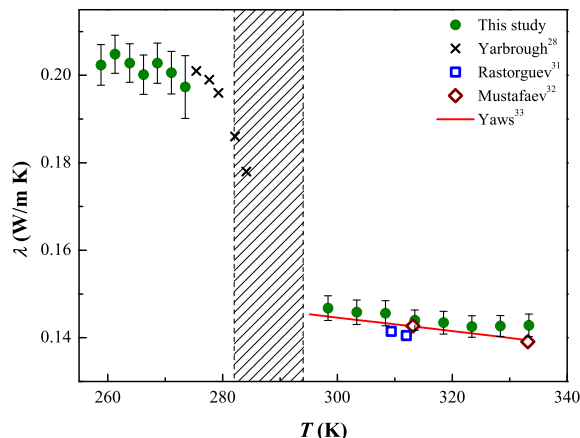
temperatures closely below a phase transition, in which case part of the heat generated in the wire is dissipated as latent heat. Therefore, the $\lambda(T)$ values obtained during the melting, near and below the phase transition temperatures, are not reported in Table 4, where only data that can be univocally attributed to a single phase is shown. For the OS ordered solid phase, Table 4 reports only data obtained at initial temperatures that are, at least, 10 K below the od phase transition, i.e., 10 K below T_{od} in Table 1. For the DS disordered solid phase, we are unable to report any reliable thermal conductivity data.

4. Discussion

As mentioned in the introduction, there is not many λ data of the investigated n-alkanes available in refereed scientific literature, particularly for the solid state, and what it is available is in some cases already rather old. A comparison was made with available data graphically, and Figs. 5–7 show for each linear alkane, as a function of temperature, the measured $\lambda(T)$ reported in Table 4 (solid circles) together with the literature values (filled symbols) and reference correlations. In Figs. 5–7 vertical lines correspond to the phase transition temperatures from DSC analysis reported in Table 1.

The number of data for the ordered solid phase published in refereed journals is very limited, and we could only find a paper by
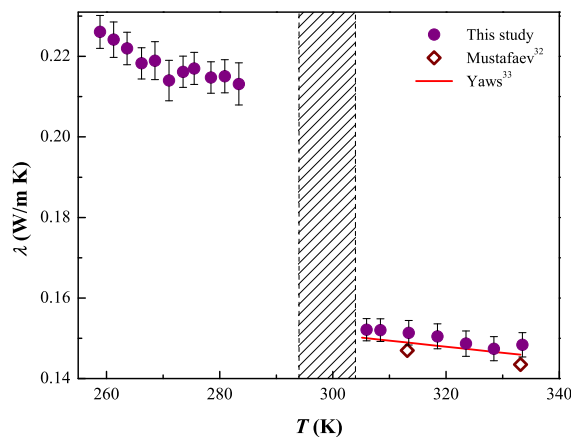
Fig. 5. Thermal conductivity measured for n-pentadecane as a function of the temperature, together with available literature data as indicated. The patterned area corresponds to the DS phase (between the two observed DSC peaks).

Fig. 7. Thermal conductivity measured for n-nonadecane as a function of the temperature, together with available literature data as indicated. The patterned area corresponds to the DS phase (between the two observed DSC peaks).

Yarbrough and Kuan [35]. Reasonable agreement with the current data is observed, particularly good for the case of n-heptadecane. However, accounting for the larger uncertainty of the current measurements for solid n-pentadecane, one can still conclude that they compare well with Yarbrough and Kuan [35] data. It should be noticed that some of Yarbrough and Kuan [35] data, which were obtained by a steady-state method, appear to refer to the disordered solid phase, for which we were unable to obtain reliable measurements.

More data is available for $\lambda(T)$ in the liquid state. Wada et al [36] measured n-pentadecane at several temperatures, as well as Bogatov et al [37] who reported up to 5 data points at atmospheric pressure in the same temperature range covered in this study. For n-heptadecane, Rastorguev and Bogatov [38] reported a couple of data points at atmospheric pressure; while in a more comprehensive work, Mustafaev [39] reported several experimental data points at atmospheric pressure for both n-heptadecane and n-nonadecane. All this available experimental data has been added to Figs. 5–7 with different symbols, as indicated. In addition to these experimental values published in refereed scientific journals, there are also available online empirical correlations proposed by Yaws [40] for liquid linear n-alkanes. For reference, we have also plotted in Figs. 5–7 as red curves the correlations proposed by Yaws [40]. In general, a good agreement is observed, within the 3% accuracy estimated for the present measurements, between literature and the data of Table 4. However, it should be also noticed that the current data for the liquid state appear to be systematically a few percent higher than the available references.

In addition to the literature data shown in Figs. 5–7, Holmen et al. [41] reported λ of n-heptadecane and n-nonadecane at their respective melting temperatures, for both the liquid and the solid phases. The λ values of Holmen et al. [41] for the liquid phase are about 50% larger than the values reported in the present paper and in other references. Furthermore, Holmen et al. [41] did not find any difference between solid and liquid λ values for n-heptadecane and n-nonadecane. Forsman and Andersson [42] reported λ data for the three alkanes investigated here, including the solid/liquid phase change region, but at a pressure of 0.03 GPa. Their results are not quantitatively comparable to the current ones, since λ of these materials strongly depends on pressure, as further confirmed by them [42]. In anyway, the data of [42] qualitatively confirm the discontinuity we find for λ between the OS and L phases. Moreover, Forsman and Andersson [42] reported some data for the intermediate DS phase that shows discontinuity with both the OS and the L phase.

Conclusions that can be reached from Figs. 5–7 as well as from the data of Table 4 are that the $\lambda(T)$ of both the liquid and solid phases increases with the number of carbon atoms in the linear alkane chain. Regarding the temperature dependence, a look at the current data displayed in Figs. 5–7 shows that $\lambda(T)$ of the liquid n-alkanes slightly decreases with increasing temperature, as it was similarly concluded by all available references. For the ordered solid (OS) phase the current measurements appear to suggest a similar behavior, however due to the larger intrinsic uncertainty, such a conclusion is less secure than in the case of the liquid phase. However, available high pressure data for this OS phase [42] confirms that this trend is robust. In spite of not being able to obtain reliable data for the intermediate DS phase, what is clearly shown in Figs. 5–7 is that thermal conductivity of the odd-numbered linear alkanes presents a discontinuity at the solid - liquid phase transition. Therefore, $\lambda(T)$ values obtained in the liquid state cannot in any reliable way be used (or extended) for the solid state. Our current research has the advantage of having shown this by measuring the same sample, in solid and liquid states, with the same setup, technique and data reduction method.

Acknowledgements

References

[1] A. Genovese, G. Amarasinghe, M. Glewis, D. Mainwaring, R.A. Shanks, Crystallisation, melting, recrystallisation and polymorphism of n-eicosane for application as a phase change material, Thermochim. Acta 443 (2006) 235–244.

[2] H. Mehling, L.F. Cabeza, Heat and Cold Storage with PCM, Springer, Berlin, 2008.

[3] X. Fang, L.-W. Fan, Q. Ding, X. Wang, X.-L. Yao, J.-F. Hou, Z.-T. Yu, G.-H. Cheng, Y.-C. Hu, K.-F. Cen, Increased thermal conductivity of eicosane-based composite phase change materials in the presence of graphene nanoplatelets, Energy & Fuels 27 (2013) 4041–4047.

[4] J.M. Khodadadi, L. Fan, H. Babaei, Thermal conductivity enhancement of nanostructure-based colloidal suspensions utilized as phase change materials for thermal energy storage:a review, Renew. Sustain. Energy Rev. 24 (2013) 418–444.

[5] NIST, http://webbook.nist.gov.

[6] C. Vélez, M. Khayet, J.M. Ortiz de Zárate, Temperature-dependent thermal properties of solid/liquid phase change even-numbered n-alkanes: n-hexadecane, n-octadecane and n-eicosane, Appl. Energy 143 (2015) 383–394.

[7] M. Dirand, M. Bouroukba, V. Chevalier, D. Petijean, E. Behar, V. Ruffier-Meray, Normal alkanes, multialkane synthetic model mixtures, and real petroleum waxes: crystallographic structures, thermodynamic properties and crystallization, J. Chem. Eng. Data 47 (2002) 115–143.

[8] H.L. Finke, M.E. Gross, G. Waddington, H.M. Huffman, Low-temperature thermal data for the nine normal paraffin hydrocarbons from octane to hexadecane, J. Am. Chem. Soc. 76 (1954) 333–341.

[9] J.F. Messerly, G.B. Guthrie, S.S. Todd, H.L. Finke, Low-temperature thermal data for n-pentane, n-heptadecane, and n-octadecane, J. Chem. Eng. Data 12 (1967) 338–346.

[10] V. Metivaud, F. Rajabalee, H.A.J. Oonk, D. Mondieig, Y. Haget, Complete determination of the solid (ri)-liquid equilibria of four consecutive n-alkane ternary systems in the range $C_{14} H_{30}$-$C_{21} H_{44}$ using only binary data, Can. J. Chem. 77 (1999) 332–339.

[11] J. Doucet, I. Denicolo, A. Craievich, X-ray study of the "rotator" phase of the odd-numbered paraffins $c_{17} h_{36}$, $c_{19} h_{40}$, and $c_{21} h_{44}$, J. Chem. Phys. 75 (1981) 1523–1529.

[12] D. Huang, S.L. Simon, G.B. McKenna, Chain length dependence of the thermodynamic properties of linear and cyclic alkanes and polymers, J. Chem. Phys. 122 (2005) 084907.

[13] K. Larsson, Arrangement of rotating molecules in the high-temperature form of normal paraffins, Nature 213 (1967) 383–384.

[14] S.R. Craig, G.P. Hastie, K.J. Roberts, J.N. Sherwood, Investigation into the structures of some normal alkanes within the homologous series $C_{13} H_{28}$ to $C_{60} H_{122}$ using high-resolution synchrotron X-ray powder diffraction, J. Mater. Chem. 4 (1994) 977–981.

[15] B. Xie, H. Shi, S. Jiang, Y. Zhao, C.C. Han, D. Xu, D. Wang, Crystallization behaviors of n-nonadecane in confined space: observation of metastable phase induced by surface freezing, J. Phys. Chem. B 110 (2006) 14279–14282.

[16] M.J. Assael, K.D. Antoniadis, W.A. Wakeham, Historical evolution of the transient hot-wire technique, Int. J. Thermophys. 31 (2010) 1051–1072.

[17] M. Khayet, J.M. Ortiz de Zárate, Application of the multi-current transient hot−wire technique for absolute measurements of the thermal conductivity of glycols, Int. J. Thermophys. 26 (2005) 637–646.

[18] J.R. Vázquez Peñas, J.M. Ortiz de Zárate, M. Khayet, Measurement of the thermal conductivity of nanofluids by the multicurrent hot−wire method, J. Appl. Phys. 104 (2008) 044314.

[19] J.M. Ortiz de Zárate, J. Luis Hita, M. Khayet, J.L. Legido, Measurement of the thermal conductivity of clays used in pelotherapy by the multi-current hot-wire technique, Appl. Clay Sci. 50 (2010) 423–426.

[20] H.S. Carslaw, J.C. Jaeger, Conduction of Heat in Solids, Oxford Univ. Press, Oxford, 1959.

[21] J. Kestin, W.A. Wakeham, Contribution to theory of transient hot−wire technique for thermal-conductivity measurements, Phys. A 92 (1978) 102–116.

[22] S.T. Ro, J.H. Lee, J.Y. Yoo, Onset of natural convection effect in a transient hot-wire system, Proceedings of the 21st Int. Conf. on Thermal Conductivity, Pleanum Press, New York (1990) 151–164.

[23] X. Zhang, S. Fujiwara, Z. Qi, M. Fujii, Natural convection effect on transient short-hot-wire method, J. Jpn. Soc. Microgravity Appl. 16 (1999) 129–135.

[24] X. Zhang, M. Fujii, Simultaneous measurements of the thermal conductivity and thermal diffusivity of molten salts with a transient short-hot-wire method, Int. J. Thermophys. 21 (2000) 71–84.

[25] R. Rusconi, W.C. Williams, J. Buongiorno, R. Piazza, L.-W. Hu, Numerical analysis of convective instabilities in a transient short-hot-wire setup for measurement of liquid thermal conductivity, Int. J. Thermophys. 28 (2007) 1131–1146.

[26] M. Freund, R. Csikós, S. Keszthelyi, G.Y. Mózes, Paraffin Products: Properties, Technologies, Applications, vol. 14, Elsevier, Amsterdam, 1982.

[27] R. Montenegro, K. Landfester, Metastable and stable morphologies during crystallization of alkanes in miniemulsion droplets, Langmuir 19 (2003) 5996–6003.

[28] D.V. Dovnar, Y.A. Lebedinskii, T.S. Khasanshin, A.P. Shchemelev, The thermodynamic properties of n-pentadecane in the liquid state, determined by the results of measurements of sound velocity, High Temp. 39 (2001) 835–839.

[29] D. Bessières, H. Saint-guirons, J.L. Daridona, Thermodynamic properties of liquid n-pentadecane, Phys. Chem. Liq. 39 (2001) 301–313.

[30] N. Dadgostar, J.M. Shaw, A predictive correlation for the constant-pressure specific heat capacity of pure and ill-defined liquid hydrocarbons, Fluid Phase Equilib. 315 (2012) 211–226.

[31] V. Ruzicka, M. Zabransky, V. Majer, Heat capacities of organic compounds in liquid state ii. C_1 to C_{18} n-alkanes, J. Phys. Chem. Ref. Data 20 (1991) 405–444.

[32] J.C. van Miltenburg, Fitting the heat capacity of liquid n-alkanes: new measurements of n-heptadecane and n-octadecane, Thermochim. Acta 343 (2000) 57–62.

[33] A.R. Gerson, K.J. Roberts, J.N. Sherwood, X-ray powder diffraction studies of alkanes: unit-cell parameters of the homologous series c_{18} h_{38} to c_{28} h_{58}, Acta Crystallogr. B47 (1991) 280–284.

[34] M.G. Broadhurst, An analysis of the solid-phase behavior of the normal paraffins, J. Res. Nat. Bur. Stand., A: Phys. Chem. 66A (1962) 241–249.

[35] D.W. Yarbrough, C. Kuan, The thermal conductivity of solid n-eicosane, n-octadecane, n-heptadecane, n-pentadecane, and n-tetradecane, Proceedings of the 17th International Thermal Conductivity Conference, Gaithersburg, Maryland, USA (1981) 265–274.

[36] Y. Wada, Y. Nagasaka, A. Nagashima, Measurements and correlation of the thermal conductivity of liquid n-paraffin hydrocarbons and their binary and ternary mixtures, Int. J. Thermophys. 6 (1985) 251–265.

[37] G.F. Bogatov, Y.L. Rastorguev, B. Grigorev, Thermal conductivity of normal hydrocarbons at high pressures and temperatures, Chem. Technol. Fuels Oils 5 (1969) 651–653.

[38] Y.L. Rastorguev, G.F. Bogatov, Thermal conductivity of n-heptadecane and n-octadecane at high pressures and temperatures, Chem. Technol. Fuels Oils 8 (1972) 176–179.

[39] R.A. Mustafaev, Thermal conductivity of higher saturated n-hydrocarbons over wide ranges of temperature and pressure, J. Eng. Phys. Thermophys. 24 (1973) 465–469.

[40] C.L. Yaws, Yaws' Handbook of Thermodynamic and Physical Properties of Chemical Compounds, Knovel, 2003. Available online.

[41] R. Holmen, M. Lamvik, O. Melhus, Measurements of the thermal conductivities of solid and liquid unbranched alkanes in the c16-to-c19 range during phase transition, Int. J. Thermophys. 23 (2002) 27–39.

[42] H. Forsman, P. Andersson, Thermal conductivity at high pressure of solid odd-numbered n-alkanes ranging from $C_9 H_{20}$ to $C_{19} H_{40}$, J. Chem. Phys. 80 (1984) 2804–2807.